ELSEVIER

Journal of Nuclear Materials 307–311 (2002) 1057–1072

journal of nuclear materials

www.elsevier.com/locate/jnucmat

Section 11. Structural ceramics and graphite

Promise and challenges of SiC_f/SiC composites for fusion energy applications

R.H. Jones [a,*], L. Giancarli [b], A. Hasegawa [c], Y. Katoh [d], A. Kohyama [d], B. Riccardi [e], L.L. Snead [f], W.J. Weber [a]

[a] *Pacific Northwest National Laboratory, MS P8-15, P.O. Box 999, Richland, WA 99352, USA*
[b] *CEA, Centre d'Etudes de Saclay, F-9119, Gif sur Yvette cedex, France*
[c] *Tohoku University, Aoba-ku, Sendai 980-8579, Japan*
[d] *Institute of Advanced Energy, Kyoto University, Gokasho, Uji, Kyoto 611-0011, Japan*
[e] *ENEA-CR Frascati, via E. Fermi, 27, I00044 Frascati (Roma), Italy*
[f] *Oak Ridge National Laboratory, Oak Ridge, TN 37831, USA*

Abstract

Silicon carbide fiber/silicon carbide matrix composites have been specified in several recent fusion power plant design studies because of their high operating temperature (1000–1100 °C) and hence high energy conversion efficiencies. Radiation resistance of the β-phase of SiC, excellent high-temperature fracture, creep, corrosion and thermal shock resistance and safety advantages arising from low induced radioactivity and afterheat are all positive attributes favoring the selection of SiC_f/SiC composites. With the promise of these materials comes a number of challenges such as their thermal conductivity, radiation stability, gaseous transmutation rates, hermetic behavior and joining technology. Recent advances have been made in understanding radiation damage in SiC at the fundamental level through MD simulations of displacement cascades. Radiation stability of composites made with the advanced fibers of Nicalon Type S and the UBE Tyranno SA, where no change in strength was observed up to 10 dpa at 800 °C, in the development of materials with improved thermal conductivity, modeling of thermal conductivity, joining techniques and models for life-prediction. High transmutation rates of C and Si to form H, He, Mg, and Al continue to be a concern.

1. Introduction

SiC_f/SiC composites offer the promise of a high-temperature fusion reactor design because of the radiation resistance of the cubic, β-phase SiC matrix, their excellent high-temperature fracture, creep, corrosion and thermal shock resistance and safety advantages arising from their low induced radioactivity and afterheat. Also, developments for other applications, such as aerospace, have driven improvements in material performance that are beneficial to fusion applications. These positive attributes of SiC_f/SiC composites have led to their being considered in the TAURO, ARIES and DREAM power plant designs.

Challenges for these materials include their thermal conductivity, radiation stability, gaseous transmutation rates, hermetic behavior and joining technology. Their radiation stability is dominated by the differential swelling between the SiC fibers, that are not fully dense or crystalline, carbon interphases and β SiC matrices. Within limits, these materials can be engineered to have select properties; therefore, much of the research in understanding their behavior and improving their performance has been focused on this aspect of their character. An overview of new understanding of the radiation behavior of SiC and SiC_f/SiC composites will be given. This includes fundamentals of radiation damage in SiC, advances in new composite materials, experiments and modeling of thermal conductivity,

* Corresponding author. Tel.: +1-509 376 4276; fax: +1-509 376 0418.
E-mail address: rh.jones@pnl.gov (R.H. Jones).

0022-3115/02/$ - see front matter
PII: S0022-3115(02)00976-5

transmutation rates, chemical compatibility and corrosion, irradiation creep and crack growth, joining technology and thermal and mechanical transient behavior. Recent experimental results and mechanistic and modeling based predictions show promise of new, improved materials.

2. Current design possibilities and needs

Silicon carbide composites (SiC_f/SiC), are being considered in future fusion power reactors because their high temperature properties ($\simeq$1000 °C), offer the potential of very high energy conversion efficiency (50% or more). SiC_f/SiC composite has been proposed as structural material for the first wall and blanket in several conceptual design studies.

2.1. Proposed blanket concepts

The most recent proposals are TAURO in the European Union, ARIES-AT in the United States, and DREAM in Japan. The first two concepts are Pb–17Li self-cooled blankets, while DREAM is cooled by 10 MPa Helium [1]. Both TAURO and ARIES-AT blankets are essentially formed by a SiC/SiC box with indirectly-cooled FW that acts as a container for the Pb–17Li which has the simultaneous functions of coolant, tritium breeder, neutron multiplier and, finally, tritium carrier. Because of the relatively low SiC_f/SiC electrical conductivity, high Pb–17Li velocity is allowed without needing large coolant pressures (<1.5 MPa). TAURO blanket is characterized by 2m-high single modules which are reinforced by SiC_f–SiC stiffeners. ARIES-AT is characterized by a coaxial Pb–17Li flow, which occurs in two 8 m-high boxes inserted one into the other. The DREAM blanket is characterized by smaller modules (0.5 m of height), each divided in three zones: FW, breeding zone and shield; neutron multiplier material (Be), tritium breeding material (Li_2O or other lithium ceramics) and shielding material (SiC) are packed in the module as small size pebbles of 1 mm-diameter for Be and Li_2O, and 10 mm for SiC. The He coolant path includes a flow through the pebble beds and a porous partition wall. These blankets allow very high coolant outlet temperatures and therefore a high energy conversion efficiency. The maximum coolant outlet temperature is 1100 °C obtained in the Pb–17Li of the ARIES-AT blanket which lead to a thermal efficiency of 58.5%.

2.2. Main assumptions for blanket designs

The TAURO, ARIES-AT and DREAM designs have been performed assuming optimistic SiC_f/SiC properties which are an anticipation of successful future R&D. The most significant assumptions are the following:

(i) The SiC_f/SiC thermal conductivity at 1000 °C and at end-of-life (EOL) conditions is 20 W/m K. This value is considerably higher than that shown by present-day SiC_f/SiC. In fact, present available data on existing industrial 3D SiC_f/SiC indicate at 1000 °C a value of 15 W/m K in the plane and of 9 W/m K through the thickness [1], without taking into account the effect of irradiation which are expected to decrease by about a factor 3 the out-of-pile value.

(ii) The maximum and minimum acceptable temperatures are respectively 1100 °C and 600 °C; these values need to be confirmed under irradiation for EOL conditions.

(iii) Compatibility between Pb–17Li and SiC_f/SiC is acceptable at 800 °C; this statement should be valid after irradiation and at Pb–17Li velocity of few m/s and should also be valid for any brazing materials in contact with Pb–17Li; available data confirm a good compatibility for static Pb–17Li at 800 °C for 3000 h.

(iv) Use of preliminary SiC_f/SiC models and design criteria are not yet validated by experiments; models and criteria currently used for metals and defined in industrial design codes (e.g., ASME, RCC-MR) are not applicable for SiC_f/SiC structures.

(v) The electrical conductivity of SiC_f/SiC is about 500 $\Omega^{-1}\,m^{-1}$; this value would allow sufficiently low MHD effects for self-cooled Pb–17Li blanket and correspond to the presently measured out-of-pile data. This result could, however, be jeopardized by Pb–17Li infiltration in the top layer of SiC_f/SiC; this infiltration could dramatically increase the wall electrical conductivity which could quickly become unacceptably high. A SiC coating on SiC_f/SiC is probably sufficient to avoid this kind of effect.

(vi) Acceptably low coolant leakage in case of He-cooling (10 MPa of pressure); very low quantity of He is tolerated in the plasma so SiC_f/SiC hermeticity need to be ensured by a reliable coating which should have the same irradiation resistance of the main structures; no experimental results are yet available to give indication about this requirement.

(vii) Possibility of manufacturing relevant shapes with appropriate thickness ranging between 1 and 6 mm. Present requirements appear achievable in present day industrial composites; however, material properties in these conditions need to be experimentally verified.

(viii) Existing methods of joining finite components with characteristics similar to the base material; good results are already available.

(ix) Acceptable structure lifetime in terms of neutron fluence and plasma-first wall interaction; a significant experimental campaign is required to define the SiC_f/SiC limits.

2.3. SiC_f/SiC thermo-mechanical model and design criteria

The proposal for using SiC_f/SiC as structural material for a nuclear component with a reasonably long lifetime is fairly recent, therefore no adequate modeling and design criteria are available yet. Some preliminary work has recently been performed [2] aiming both to identify appropriate models available in the aerospace research field and to theoretically define sound design criteria to improve the design thermo-mechanical analyses.

2.3.1. Modeling

SiC_f/SiC composites exhibit a complex nonlinear behavior combining brittle damage, residual strains and opening-closing of microcracks. These composites present different properties, and therefore different strengths, for different loading directions; moreover, tensile and compression strengths are very different. Under loading, the interaction of fibers and matrix lead at first to matrix microcracking, then to matrix/fiber decohesion, followed by opening of the microcrack and finally to fiber failure. This sequence corresponds to an initial isotropic behavior in plane and then to a crack growth perpendicular to the fibers depending on the load direction. A relatively simple model, able to take into account such a behavior and based on continuum damage mechanics which consider the composites as a continuous media, has been implemented in the FEM code CASTEM. Significant improvements on the results have been obtained when compared with models used for metals [1]. On the other end, damage description has been limited to scalar variables that is appropriate when damage is oriented in the fiber direction but not satisfactory when damage is loading oriented. A substantial effort is still required to develop and implement this for a complete design model.

2.3.2. Design criteria

To avoid degradation of the composite physical properties, the elastic limit must be used as the maximum allowable stress. On the other hand, one of the most attractive characteristics of SiC_f/SiC composites is that they are damage-tolerant, that is, they are capable of accommodating a high degree of deformation because of crack arrest phenomena driven by the interface between fibers and matrix. In principle, it can be assumed the limit for matrix microcracking saturation (beginning of fiber/matrix debonding) as the maximum allowable tensile stress. The actual failure limit can instead be assumed as the maximum allowable compressive stress since no damage is observed under compression. The number of fibers through the thickness of the composite is usually lower and their arrangement different. So, if one can accept the uncoupling of stresses in plane and stresses through the thickness, the former can be evaluated using the Von Mises criteria, while the latter corresponds to the measured rupture value. Taking into account the above remarks, for compressive stresses the limit is the rupture limits while for tensile stresses the limit is the elastic limit. A margin of about 20% may be allowable on the elastic limit.

For example, in the case of the TAURO blanket, based on the CERASEP® composites produced by SNECMA, the following limits have been assumed:

- for normal stresses through the thickness, 110 MPa for tensile stresses (roughly corresponding to the matrix tensile resistance limit outside the composite) and 420 MPa for compressive stresses (rupture limit for CERASEP N2-1);
- for shear stresses through the thickness, 44 MPa (assumed rupture limit, to be confirmed);
- for stresses in plane, 145 MPa for tensile stresses (beginning of fiber/matrix debonding) and 580 MPa for compressive stresses (rupture limit measured on the CERASEP® N2-1). It appears clear that this design criteria proposal is very preliminary; it needs to be further evaluated both theoretically and, more important, experimentally through a systematic specific experimental campaign.

3. Promise of SiC_f/SiC composites

Composite materials made from continuous fibers of SiC, can be woven into several variant fabric architectures and the matrix formed with a variety of infiltration methods. The β-phase of SiC has been shown by numerous studies [1] to have a saturation swelling value of about 0.1–0.2% at 800–1000 °C. This suggests that composites of SiC_f/SiC have the potential for excellent radiation stability. The continuous fiber architecture, coupled with engineered interfaces between the fiber and matrix, provide excellent fracture properties and fracture toughness values on the order of 25 MPa $m^{1/2}$. The strength and fracture toughness are independent of temperature up to the limit of the fiber stability. With improvements in fiber stability these materials exhibit excellent mechanical properties to at least 1200 °C. Also, these fiber/matrix microstructures impart excellent thermal shock and thermal fatigue resistance to these materials so plasma discharge and start-up and shutdown cycles should not induce significant structural damage. In oxygen bearing environments, SiC will form a protective layer of SiO_2 that greatly retards further

oxidation. Therefore, SiC_f/SiC composites have the potential for excellent oxidation resistance in $He + O_2$ environments.

4. Challenges of engineering the properties of SiC_f/SiC

Given the positive attributes of SiC_f/SiC composites, they would be the obvious first choice for structural applications in fusion energy systems if there were no issues in their use. However, there are some unresolved issues associated with their use as outlined in Table 1. Considerable progress has been made in understanding these issues and in some cases improvements have been made. Since the properties of these composites are engineerable, there is the potential, to some extent, to engineer around these issues. The purpose of this paper is to summarize some of the understanding and improvements made in these materials.

5. Fundamentals of radiation damage in SiC

5.1. Defect formation energies

Density functional theory (DFT), based on the pseudopotential plane-wave method within the framework of the local density approximation (LDA), has been used to study the formation and properties of native defects in 3C–SiC (cubic SiC), as described in detail elsewhere [3–5]. The formation energies for vacancies, antisite defects and interstitials in 3C–SiC are summarized in Table 2. Two types of vacancies form, namely C and Si vacancies. In addition, two types of antisite defects are formed by atoms located on the wrong sublattice. For interstitial defects, there are ten possible configurations, four tetrahedral and six dumbbell (split) configurations. It is found that the most stable configurations for C interstitials are C–C and C–Si split interstitials along the $\langle 100 \rangle$ and $\langle 110 \rangle$ directions, which suggest that the C interstitials should migrate from sublattice to sublattice. The most stable configuration for Si interstitials is in a tetrahedrally-coordinated interstitial site surrounded by C atoms on the C sublattice. Ongoing theoretical and computational studies of the migration of these stable defect configurations will yield the necessary parameters to model radiation damage processes at higher temperatures and over longer time scales in SiC using rate-theory approaches or kinetic Monte Carlo methods.

Table 1
Critical issues associated with the use of SiC_f/SiC composites in nuclear environments

Primany issues	Secondary issues
Thermal conductivity	Chemical compatibility (He)
Radiation stability	+ Carbon interfaces
+ Fibers-polymer derived	Thermal fatigue and shock
Interphases-C, porous	Lack of a database
+ Matrices-CVI and polymer impregnated	Long-term thermal stability
Transmutations	Design codes
Hermetic behavior	
Joining technology	
Chemical compatibility (Pb–Li)	

Table 2
Defect formation energies in 3C–SiC [4]

Defect type	Formation energy (eV)
V_C	5.48
V_{Si}	6.64
C_{Si}	1.32
Si_C	7.20
C_{TC}	6.41
C_{TS}	5.84
Si_{TC}	6.17
Si_{TS}	8.71
C^+–Si$\langle 100 \rangle$	3.59
C^+–C$\langle 100 \rangle$	3.16
C–$Si^+\langle 100 \rangle$	10.05
Si^+–Si$\langle 100 \rangle$	9.32
C^+–C$\langle 110 \rangle$	3.32
C^+–Si$\langle 110 \rangle$	3.28

5.2. Damage production and accumulation

Molecular dynamics (MD) simulations of displacement cascades and cascade overlap events have been performed using a modified version of the code MOLDY [6], with either constant volume or constant pressure and periodic boundary conditions. Details of the MD simulations and interatomic potentials employed are described elsewhere [7–10].

The short cascade lifetime in SiC is illustrated in Fig. 1, where the numbers of interstitials and antisite defects produced in a 10 keV Si cascade are shown as a function of time. The number of interstitials and vacancies (not shown) reaches a peak at about 0.1 ps and then decreases due to defect recombination [7,9,10]. The defect concentrations attain steady state values after about 0.4 ps. The cascade lifetime has been found to be slightly longer (about 0.7 ps) for a 50 keV Si PKA in SiC [7,9]. These lifetimes are about an order of magnitude smaller than the values reported for metals using similar PKA energies [6,11].

The results from MD simulations [10] for the net displacements and antisite defects produced by a 10 keV Si primary knock-on atom (PKA) are shown in Fig. 2 as a function of PKA energy. The number of net displacements is defined as the sum of the total number of interstitials (or vacancies) and antisite defects. The

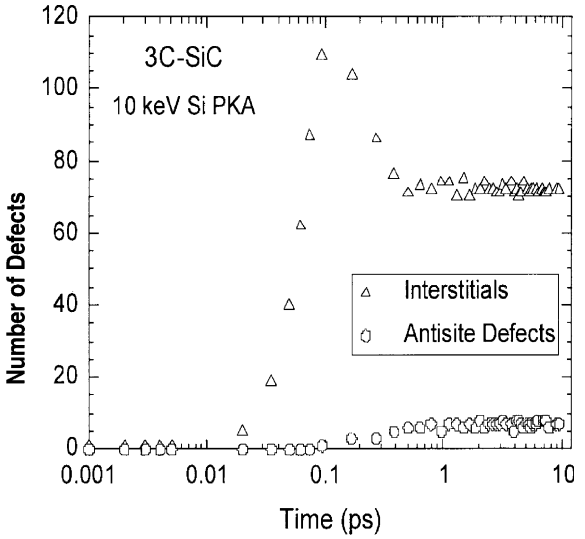

Fig. 1. Number of interstitials and antisite defects produced in a 10 keV Si cascade as a function of time [10].

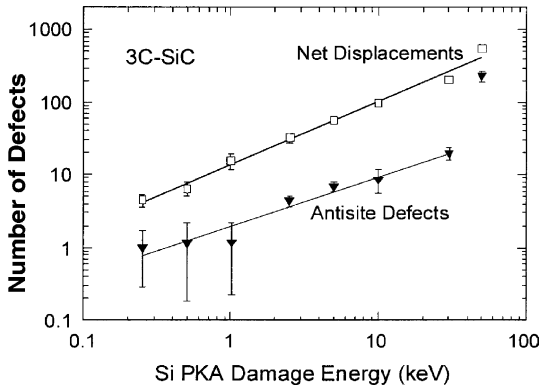

Fig. 2. Net displacements and antisite defects produced as a function of Si PKA damage energy [10].

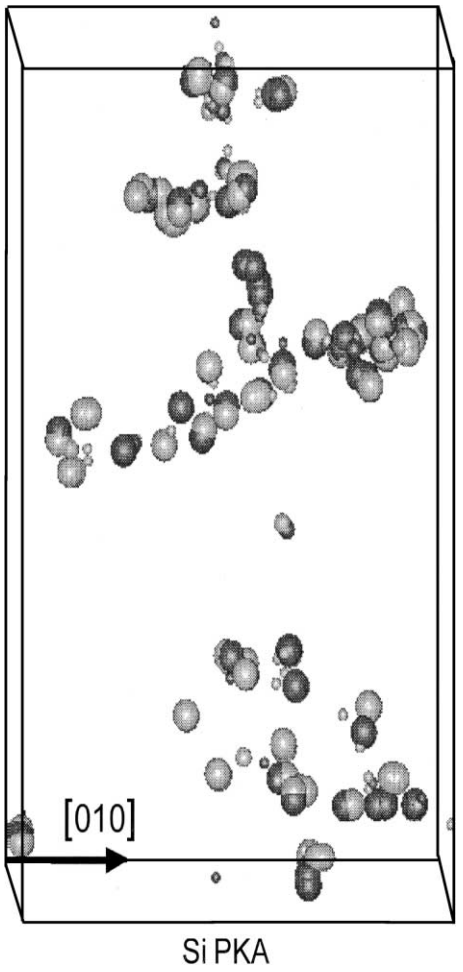

Fig. 3. MD simulation of primary damage state in SiC at 300 K due to a 10 keV Si PKA [8]. The Si and C defects are dark and light gray, respectively, and the interstitials, antisite defects and vacancies are given by large, medium, and small spheres, respectively.

number of C displacements is much larger than the number of Si displacements, which is consistent with recent experimental observations [5]. Similar behavior is observed for C PKAs. Antisite defects are produced by nearest-neighbor replacements during the collisional phase and some random interstitial-vacancy recombination during the subsequent relaxation phase.

MD simulations, as illustrated in Fig. 3, have also shown that Si PKAs generate only small interstitial clusters, with most defects being isolated single interstitials and vacancies distributed over a large region [8,12,13]. These predictions are in agreement with the interpretation of the experimental results on disordering behavior in SiC, as shown in Fig. 4, where the relative disorder on the Si sublattice in SiC at the damage peak is shown as a function of dose in displacements per atom (dpa) for irradiation with 550 keV Si^+ ions at 190 K [12–14]. The solid curve (Fig. 4) is based on the direct-impact/defect-stimulated model for amorphization [15], where point defects, such as interstitials and antisite defects, stimulate the growth of amorphous nuclei (or defect clusters) produced directly in a displacement cascade. As the dose increases, cascade superposition and defect-stimulated growth at crystalline-amorphous interfaces become more probable. The relative ratio of direct-impact and defect-stimulated cross sections from the model fit to the data for Si are consistent with those derived from the MD simulations based on relative cluster distributions [12].

MD methods with 10 keV Si PKAs have been employed to simulate cascade overlap, damage accumulation and amorphization processes in 3C–SiC. In this

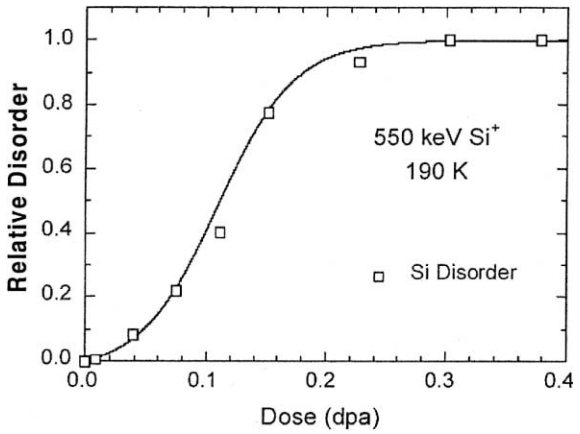

Fig. 4. Relative disorder on the Si sublattice at the damage peak as a function H–SiC irradiated with 550 keV Si^+ ions at 190 K [12–14].

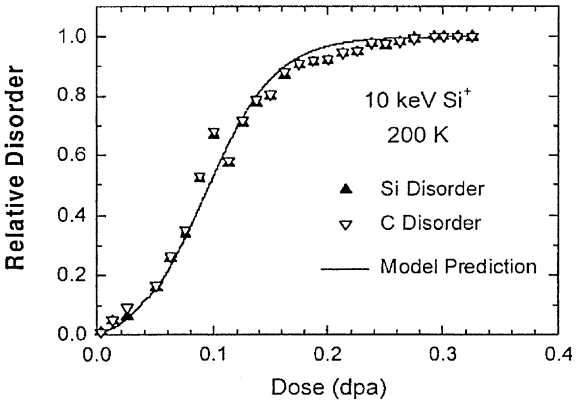

Fig. 5. Relative disorder in SiC based on MD simulations [16–18].

simulation study, 10 keV Si cascades, similar to those in Fig. 3, were randomly overlapped at 200 K in an MD simulation cell containing 40 000 atoms until a fully disordered state was achieved after 140 cascades [16–18]. At low doses, damage is dominated by single interstitials and small clusters consisting of interstitials and antisite defects, and their concentration increases with increasing dose. The coalescence of small and large clusters at higher doses is an important mechanism leading to amorphization in SiC, and the homogeneous nucleation of small clusters at low doses is consistent with the homogeneous amorphization process that is observed experimentally by high-resolution TEM [19]. Under these conditions, the primary driving force for irradiation-induced amorphization is the accumulation of both interstitials and antisite defects. The relative disorder from the MD simulations exhibits a sigmoidal dependence on dose, as shown in Fig. 5, that is in good agreement with the experimental measurements for 550 keV Si^+ irradiation (Fig. 4). The interpretation of the MD results is consistent with the direct-impact/defect stimulated model for amorphization, where the production of interstitials and antisite defects stimulates amorphous growth at crystalline-amorphous interfaces. The model fit shown in Fig. 5 is based on the average relative cross sections determined previously for single 10 keV Si cascades [12]. High-resolution TEM image simulations of specific damage states in the MD simulation cell have been performed to reveal the change in microstructural features with increasing dose from cascade overlap [17]. The microstructural evolution in the MD simulations is very similar to that observed previously in experimental HRTEM images obtained from ion-irradiated 3C–SiC [19]. Likewise, the swelling and stored energy determined as a function of dose from cascade overlap in the MD simulations are in good agreement with experimental measurements [18]. Thus, the good agreement between MD simulations and experimental results provides atomic-level insights into the interpretation of radiation damage processes in SiC. Ongoing MD simulations on cascade annealing and defect migration in SiC will yield new atomic-level understanding of the temperature dependence of radiation damage processes in SiC.

6. Recent advances in SiC_f/SiC performance

6.1. New materials

6.1.1. Composites with advanced fibers

Composites produced with the advanced fibers, Hi-Nicalon Type S and Tyranno-SA have been irradiated and the test results are presented and compared to other data in Fig. 6 [20–29]. Comparison is made to both monolithic SiC and composites made with Ceramic Grade-Nicalon and Hi-Nicalon fibers. The results cover a range of temperatures but the trend of the irradiated to unirradiataed ultimate strength, S_u^{irrad}/S_u^{unirr}, clearly shows that composites with the advanced fibers Hi-Nicalon Type S and Tyranno SA showed no loss in strength up to a dose of 10 dpa. The results of Price [28,29] and Jones et al. [22] give some support to the possibility that the strength of irradiated advanced fiber material could remain unchanged up to at least 10 dpa and perhaps higher. Further advances will likely require tailoring the interface swelling characteristics to compensate for differential swelling between the fiber and matrix. Advanced interface developments that could provide this tailoring have been reported by Snead [27] and they include multilayer SiC/C interfaces and porous or pseudo-porous SiC interfaces. An example of a multilayer interface is shown in Fig. 7 and the resulting room temperature bend strengths are given in Fig. 8.

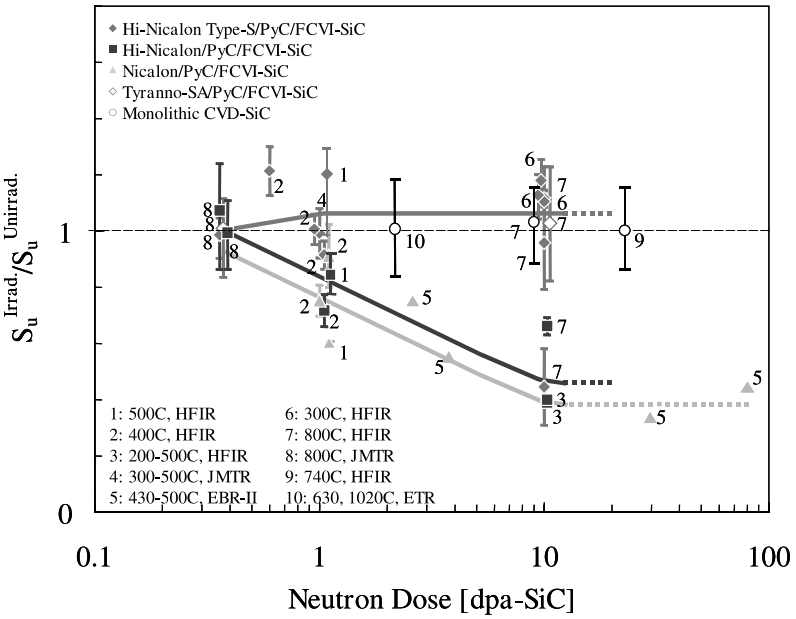

Fig. 6. Relative strength, irradiated/unirradiated, for SiC_f/SiC composites versus radiation dose.

These results show that it is possible to achieve significant bend ultimate strengths for unirradiated SiC_f/SiC composites with either multilayer and pseudo-porous interfaces but that the radiation stability for a composite with Hi-Nicalon is better with the multilayer than the pseudo-porous interface.

6.1.2. New SiC_f/SiC composites by transient liquid phase sintering process

The LPS process, which has been a common technique in producing monolithic silicon carbide and other ceramics at relatively low costs, was successfully applied to matrix densification for SiC_f/SiC composites for the first time. The lab-grade materials with uni-directional reinforcement exhibits typically 700 MPa in three-point flexural strength and pseudo-ductile fracture mode with a good fiber pull-out. Tensile strength tests, both at room and at elevated temperature, and fracture toughness evaluation are in progress. The composites are almost fully-dense, with very minor porosity within intra-fiber-bundles. Thermal conductivity and hermeticity data will soon be available. Larger scale production and complex shaping are presently being attempted.

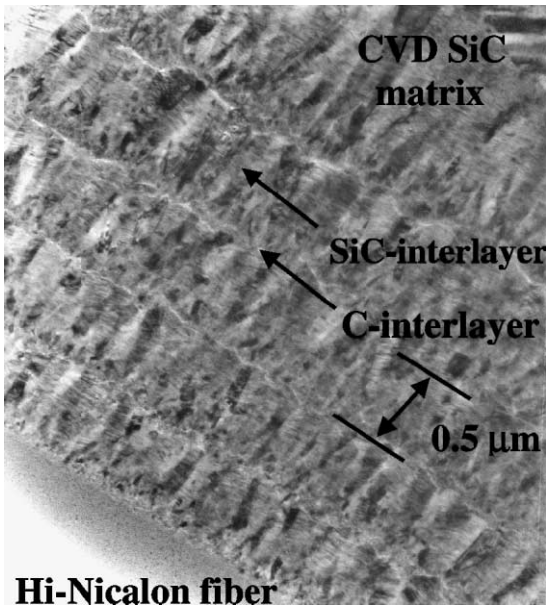

Fig. 7. Multilayer SiC interphase with thin pyrolitic layer applied followed by SiC interlayers.

6.2. Thermal conductivity: modeling based guidance to performance improvements

A major issue to be considered when using SiC_f/SiC in a high-temperature neutron radiation environment, or in other non-radiation environments where components or structures are subjected to a high heat flux, is the expected in-service behavior of its effective transverse thermal conductivity, K_{eff}. Knowledge about the expected range of K_{eff} is necessary to optimize SiC_f/SiC configurations for their intended uses. Several modeling

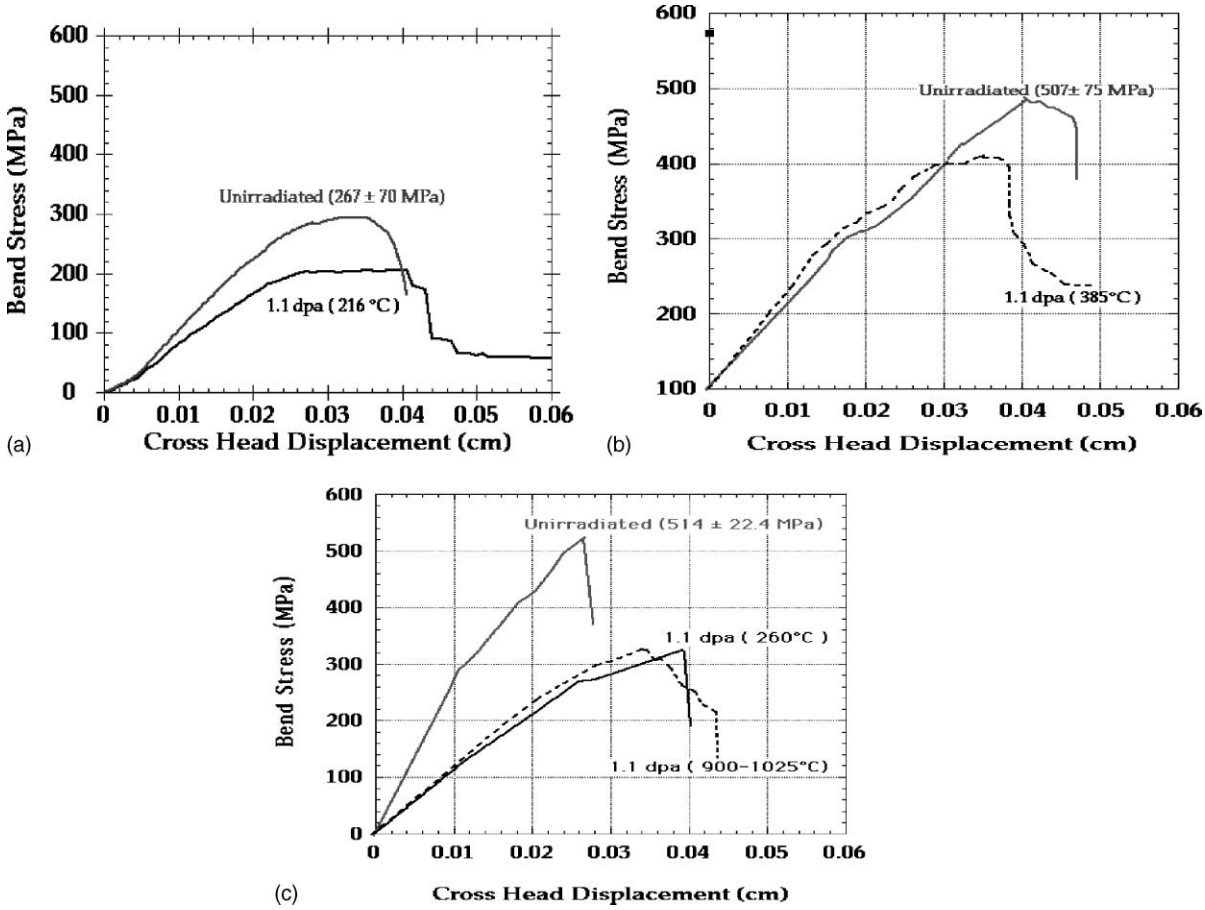

Fig. 8. Bend-displacement curves for SiC_f/SiC with (a) pyrolytic C, (b) multiplayer, and (c) porous interfaces.

studies have shown how K_{eff} depends upon constituent fiber and matrix thermal conductivity values, and their volume fractions and distributions [30–33]. However, many experimental measurements have indicated that interfaces between fibers and matrices in a composite introduce a thermal barrier that may reduce K_{eff} [34–37]. Furthermore, K_{eff} may be altered by physical changes of the interface and even the surrounding atmosphere. As with mechanical behavior, to attain desired thermal behavior of SiC_f/SiC proper attention needs to be given to the design of the interphase and the control of interfacial thermal effects. Classical composite models recently have been updated to include the effect of interfacial thermal barriers [38]. Interfacial thermal barriers are quantitatively characterized by a value called the interfacial conductance, which includes the effect of imperfect matching of surfaces at an interface as well as the effect of interfacial gaps brought about by debonding of the fiber from the matrix or microcracking within the fiber coating [38].

For fiber-to-matrix conductivity ratios (r) less than 10 ($r < 10$) and for fiber volume fractions, (f) $\leqslant 0.5$, the Hasselman–Johnson (H–J) model predictions given by Eq. (1) deviate from numerical FEM results by less than 5%. By Eq. (1), for dispersed fibers in a matrix the effective transverse thermal conductivity (K_{eff}) is primarily controlled by the thermal conductivity of the continuous matrix phase (K_m) and the interfacial conductance (h). A simple thermal barrier model was introduced to describe 'h' and the gaseous and direct contact components ($f_g h_g$ and $f_d h_d$, respectively). Values of h determined by Eq. (2) for a uniaxial Hi-Nicalon™ fiber/amorphous SiC matrix composite in vacuum, argon and helium compared favorably with values estimated by the simple thermal barrier model. Reasonable agreement between numerical FEM and experimental results with H–J model predictions suggest that K_{eff} for a SiC_f/SiC composite with fiber volume fractions $f \leqslant 0.4$ and with simple unidirectional or cross-ply fiber architecture are well described by Eq. (1) below:

$$K_{\text{eff}} = K_{\text{m}}[(K_{\text{f}}/K_{\text{m}} - 1 - K_{\text{f}}/ah)V_{\text{f}} + (1 + K_{\text{f}}/K_{\text{m}} + K_{\text{f}}/ah)] \times [(1 - K_{\text{f}}/K_{\text{m}} + K_{\text{f}}/ah)V_{\text{f}} + (1 + K_{\text{f}}/K_{\text{m}} + K_{\text{f}}/ah)]^{-1}, \quad (1)$$

where h is the effective interfacial conductance; K_{m} and K_{f} are the thermal conductivity values of the matrix and fiber constituents; and V_{f} and a are the fiber volume fraction and radius, respectively.

For a woven 2D-SiC_f/SiC composite, the localized effects of dense fiber packing within individual tows ($f \leqslant 0.6$) and the occurrence of many direct fiber–fiber contacts at the numerous fiber bundle crossover points will introduce positive deviations from Eq. (1). However, the analytic solution expressed by Eq. (1) should be very appropriate to examine thermal conductivity degradation induced in these composites by neutron radiation or by other mechanical or environmental treatments. If a 2D-SiC_f/SiC composite with initially high K_f- and h-values were irradiated, K_{eff} could easily be reduced by a factor of five or six due to the degradation of the interface conductance and the matrix conductivity.

To further examine this issue, the effects of temperature and irradiation on K_{eff} were predicted for a hypothetical 2D-SiC_f/SiC composite made with high conductivity Tyranno SA™ fiber, a thin (0.2-μm) PyC fiber coating and a CVI-SiC matrix. For example, it was predicted for this composite that K_{eff} would decrease from 34 W/m K before irradiation to <6 W/m K (at 200 °C) after irradiation at 200 °C. Similarly, K_{eff} would decrease from 26 W/m K before irradiation to <10 W/m K (at 1000 °C) after irradiation at 1000 °C.

6.3. Transmutation rates

Transmutation calculations were performed using the REAC-3 code for pure SiC irradiated in the neutron spectrum of the first wall of the ARIES-IV conceptual fusion energy device. The ARIES-IV first wall has a total neutron flux of 3.6×10^{15} n/cm^2 s and a fast flux ($E > 0.1$ MeV) of 1.9×10^{15} n/cm^2 s. Calculations were performed for a continuous irradiation of up to 12 effective full power years (efpy) to a total neutron dose of 1.37×10^{24} n/cm^2. The elemental composition of the material is not significantly affected by the post-irradiation decay of radioactive isotopes, since they are either too short-lived or too long-lived to affect the composition over a reactor lifetime.

6.3.1. SiC burn-out

In this neutron spectrum, Si burns out somewhat more rapidly than C, Fig. 9. Si burns out at a rate of about 0.0047/efpy. A 3% burnout of SiC has been suggested as a design limit for SiC composites. In ARIES-IV, a 3% burnout occurs in about 6.5 efpy (total neutron fluence 7.4×10^{23} n/cm^2). The differing burnout rates of Si and C result in an excess concentration of carbon totaling about 3500 appm after 6.5 efpy. The Si and C burnout rates are constant, and the excess C increases at the rate of 540 appm excess C/efpy.

6.3.2. Impurity burn-in

The most abundant transmutation products, which burn-in at constant rates, Fig. 10, are listed in Table 3. After 6.5 efpy, although 3% of the SiC burns out, the concentration of transmutant atoms totals almost 8%. This is because many transmutation reactions create

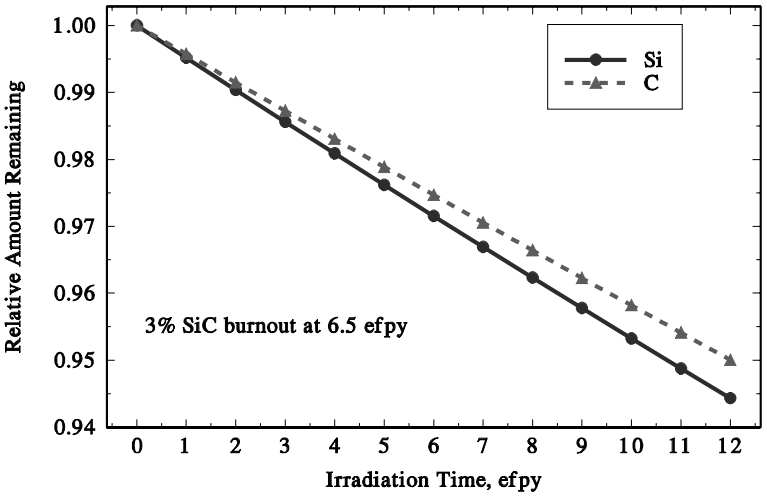

Fig. 9. The burnout of Si and C in SiC irradiated in ARIES-IV first wall as a function of dose in efpy.

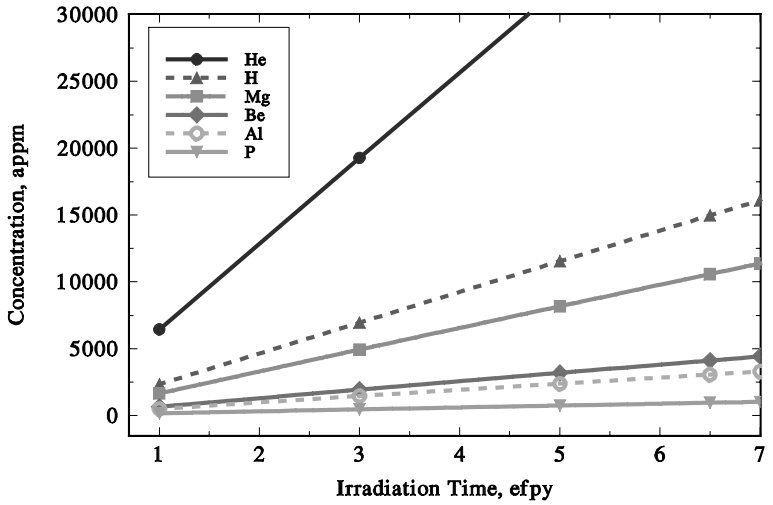

Fig. 10. Concentrations of transmutation products in SiC irradiated in ARIES-IV first wall as a function of irradiation time in effective full power years.

Table 3
Transmutation products – SiC

Element	Burn-in rate (appm/efpy)	Concentration at 6.5 efpy (at.%)
He	6384	4.2
H	2307	1.5
Mg	1630	1.1
Be	632	0.4
Al	469	0.3
P	146	0.1

additional H or He atoms, which causes the total number of atoms in the system to increase.

Several other elements burn-in through two-step transmutations, so they accumulate nonlinearly as the square of the irradiation time. Their concentrations are relatively small compared to the transmutants discussed above, Fig. 11. The concentrations of elements produced by two-step transmutations after 6.5 efpy are listed in Table 4.

Of the elements identified as transmutation products in this report, only Al and Na are also considered as

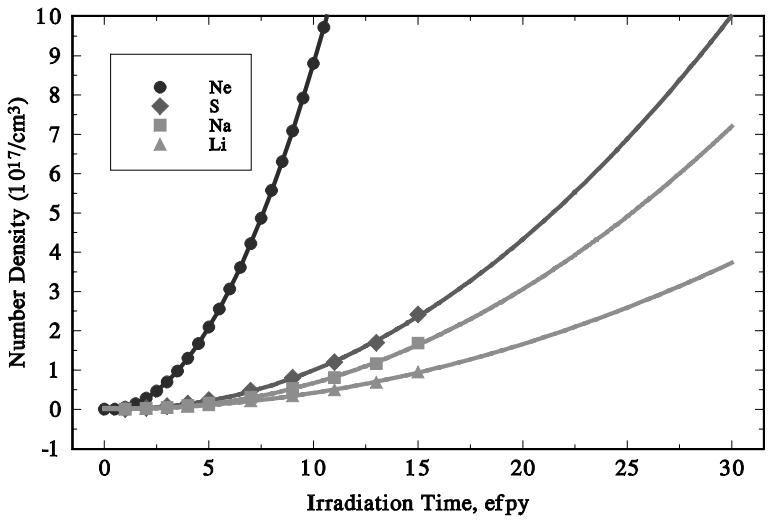

Fig. 11. Number density of transmutation products in SiC that result from multiple interactions of a nucleus with neutrons in the ARIES-IV first wall as a function of irradiation time in effective full power years.

Table 4
Transmutations from two-step reactions

Element	Concentration at 6.5 efpy (appm)
Ne	78
S	8
Na	7
Li	4

possible intrinsic impurities in unirradiated SiC. After only one efpd the concentrations of Al and Na due to transmutations are greater than typical concentrations of these elements as impurities. Thus, transmutations are responsible for creating an additional set of radiation-induced impurities, having dose-dependent concentrations, that is entirely different from the intrinsic impurities.

6.4. Chemical compatibility and corrosion

Chemical compatibility and corrosion issues for the application of SiC in gas, liquid metal and molten salt cooled fusion reactors have been reviewed by Jones [36]. For a gas-cooled system, chemical compatibility with solid breeders and reactions of small concentrations of O_2 in a gas coolant are the key issues. Sample et al. [37] reviewed the chemical reactions of concern between SiC and solid breeders and noted that lithium silicate, zirconate and aluminate materials all reacted with SiO_2 on the surface of the SiC. The SiO_2 resulted from the reaction of trace amounts of O_2 in the environment with SiC; however, the Li_2CO_3 impurity content of the Li_4SiO_4 induced the greatest reaction with SiC. Trace quantities of O_2 in the coolant gas can also react with the fiber/matrix interfacial layer. Analysis of this effect has been summarized by Jones et al. [38,39] and its effect is included in the crack mechanism map described below.

Liquid Pb–Li is considered as the coolant and breeding material for the TAURO and ARIES-AT reactor designs. Fenici and Scholz [40] reported that CVI SiC_f/SiC composite samples were stable in a static solution of Pb–17Li at 800 °C for up to 1500 h. They concluded that SiC should be very stable in this environment because the free energy change for the following reaction is about +99 kJ/mol over the temperature range of 700–900 °C:

$$2SiC + 2Li \rightarrow Li_2C_2 + 2Si. \quad (2)$$

Kleykamp [41] showed that the free energy change is only +24 kJ/mol for the reaction given by Eq. (2) at 823 °C and becomes negative at 1000 °C. Terai et al. [42] also reported that SiC_f/SiC composite and monolithic SiC exhibited excellent stability in Pb–16Li at 300 and 500 °C for 666 h exposure. The largest weight loss reported was 1.5% for a SiC_f/SiC composite with Hi-Nicalon fibers, pyrolytic carbon fiber/matrix interface and matrix produced by the PIP process. Two other composite materials showed a factor of 10 less weight loss. In contrast, samples immersed in Li at 427 °C for the same period of time were totally dissolved with the exception of a high-purity, monolithic CVD SiC. These results are consistent with the conclusion of Fenici and Scholz [40] regarding the free energy change for the reaction given by Eq. (2). Reactions with other phases such as residual Si and C are a likely reason for the high reactivity of the other samples tested. In a review of temperature limits for fusion reactors, Zinkle and Ghoniem [43] concluded that the limits for SiC in Li, Pb–17Li and Sn–Pb–Bi are <550 °C, >800 °C and >760 °C, respectively. The current corrosion results in Pb–Li are limited to static immersion tests but the blanket material will be in contact with the flowing coolant where combined erosion–corrosion effects could occur. Therefore, effect of coolant flow rate must be evaluated.

6.5. Crack growth mechanism map and mechanism based life predictions: thermal and irradiation enhanced creep, and oxygen pressure effects

A dynamic crack-growth model, developed to predict crack growth in ceramic composites containing creeping fibers in an elastic matrix, has been used to predict effects of temperature, time, oxygen pressure, and irradiation on crack growth of SiC_f/SiC composites [44,45]. Mechanics for frictional bridging and both linear and nonlinear fiber-creep equations are used to compute the dynamic crack extension. Discrete, two-dimensional fiber bridges are employed, which allows separate bridge 'clocks', to compute crack-growth rates for composites containing fibers undergoing any variety of time-dependent processes. The approach to modeling time-dependent bridging controlled by fiber creep starts by expressing the crack-opening displacement as a function of time and position along the crack face for both applied and bridging tractions. The force or stress on each bridge as a function of time and position is then solved. The bridges conform to the mechanics of frictionally bonded fibers and follow an appropriate parametric fiber-creep law, which can be either linear or nonlinear in stress and time. Thermal creep of polymer derived ceramic fibers is often nonlinear, or viscous-like, in time and stress, but oxygen causes the crack growth to be linear in time. Reaction rate equations were determined from experimental measurements for the reaction of oxygen with the C interphase. The interphase recession rates were modeled from these reaction rates. The reaction rates for oxygen with SiC to form SiO_2 were obtained from the literature. Irradiation creep of these same fibers also appears to be linear in both time (dose) and applied stress, Fig. 12. Accordingly, a standard

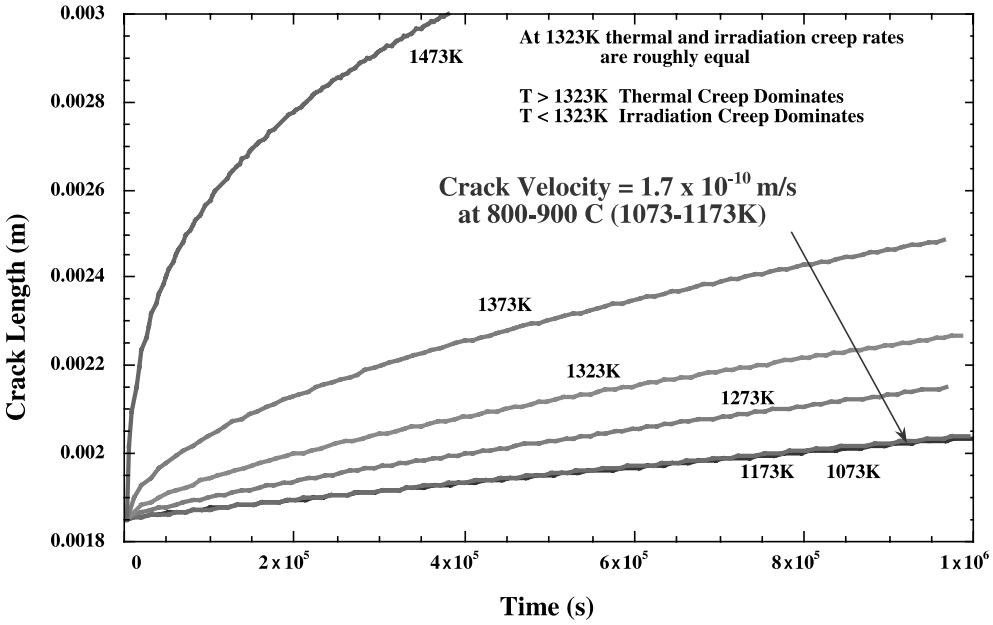

Fig. 12. Calculated crack length versus time, showing effects of irradiation creep.

thermal creep equation and a simple irradiation creep equation suitable for SiC-based fibers were used to generate some model results for two test temperatures, 1273 and 1373 K (1000 and 1100 °C). The thermal creep equation has an activation energy of about 600 kJ/mol [45]. The irradiation creep equation assumes a temperature independent regime below 1173 K (900 °C) and an activation energy of 50 kJ/mol [45] for temperatures greater than 1173 K. The creep rate is linear in dose rate and stress. We observe that irradiation creep of the fibers dominates the fiber deformation process for temperatures below 1273 K (1000 °C) but thermal creep dominates at higher test temperatures.

The subcritical crack growth mechanism of SiC_f/SiC composites is a function of temperature, stress, environment, loading mode and time as well as other secondary variables. The crack growth mechanisms include oxidation embrittlement (OE) in high oxygen containing environments, interphase removal (IRM) in intermediate oxygen containing environments, fiber relaxation (FR) and fiber irradiation creep relaxation (FIR) in low oxygen containing environments, stress-rupture (SR) of the fiber at high temperatures and viscous sliding at high temperatures and oxygen concentrations, Fig. 13. The transition between these mechanism is also a function of temperature, stress and time.

Experimental weight loss and crack growth data were used to conclude that the oxygen-enhanced crack growth of SiC_f/SiC composite occurs by more than one mechanism depending on the experimental conditions. An OE mechanism operates at temperatures below a critical value ($T < T_g$) and at high oxygen concentrations; an IR mechanism operates a lower temperatures and low oxygen concentrations. The IR mechanism may operate at short times, with a transition to the OE mechanism at longer times if the glass layer becomes sufficiently thick and the stress is low enough that failure does not occur first. The OE results from the reaction of oxygen with SiC to for SiO_2 on the fiber or the matrix. The fracture stress of the fiber is decreased it this layer is thicker than a critical value ($d > d_c$) or if it is thick enough to bridge between the fiber and matrix across the interface and the temperature is below a critical value ($T < T_g$) such that a sharp crack or stress concentration can be sustained in the layer. Other possible, but not demonstrated, OE mechanisms include: (1) viscous sliding (VS) of the fiber from glass-phase formation in the fiber-matrix interface, and (2) fiber-strength reduction by reaction with oxygen. The IR mechanism results from the oxidation of the fiber/matrix interfacial layer and the resulting relaxation of the bridging fibers. Interface removal contributes to the creep relaxation of the fiber. The IR mechanism occurs over a wide range of temperatures for $d < d_c$ and may occur at $T > T_g$ and $d > d_c$. The IR mechanism has only been observed in SiC_f/SiC composites with either carbon or BN as the fiber-matrix interface material.

The slowest crack growth rate and hence the longest lifetime for SiC_f/SiC in a $He + O_2$ environment is in the FR dominant regime. Even with some oxygen in the environment it could be possible for the crack velocity in SiC/SiC to be slow enough that a component will not fail

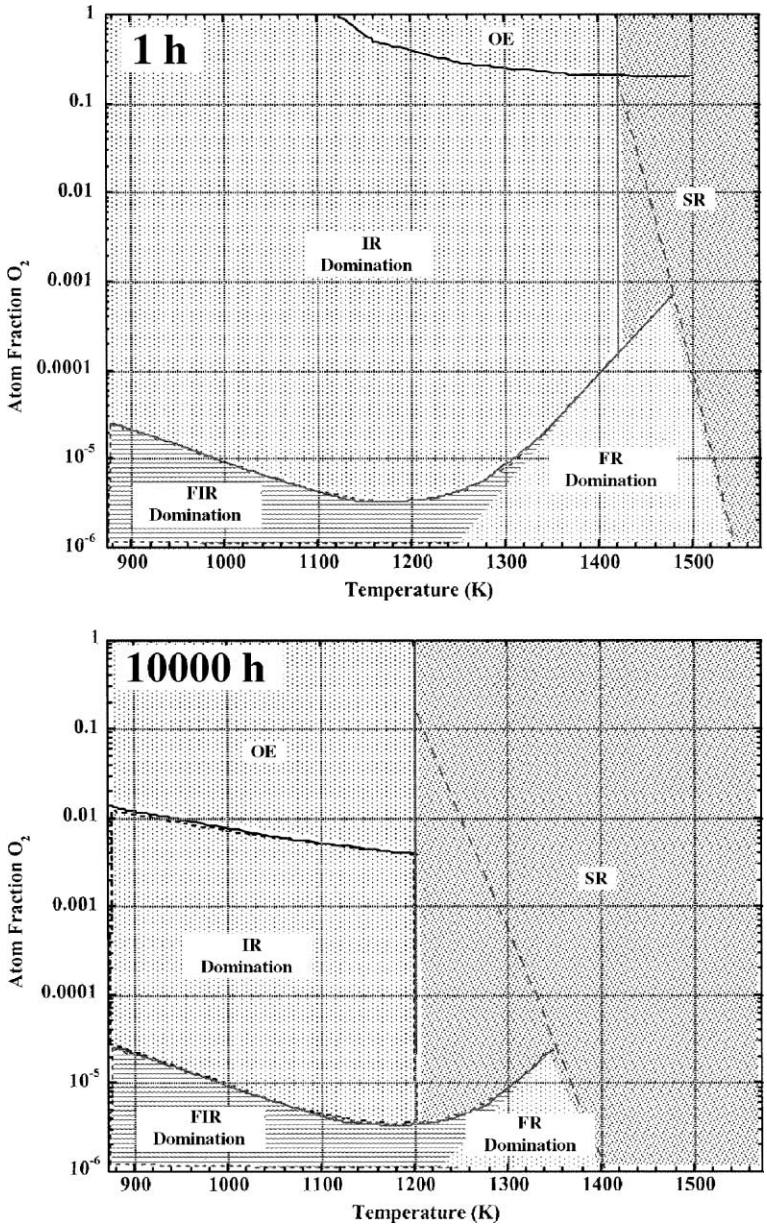

Fig. 13. Crack growth mechanism maps for SiC_f/SiC composites with pyrolytic C interfaces after 1 and 10 000 h of exposure. The crack growth mechanisms are: OE, IR, SR, FR and FIR.

for the life of the reactor. For example, the dynamic crack growth model predicts a lifetime of about 50 years in a He coolant containing 0.5 appm oxygen for cracks growing in the IR dominant regime shown in Fig. 13. The effect of irradiation creep on the FR process (designated the FIR dominant regime) is uncertain since this effect is relatively new and additional data are needed to fully evaluate its effect on crack growth; current data clearly suggests that irradiation will produce fiber creep at temperatures substantially below the thermally activated creep regime.

6.6. Joining technology

To enable the use of SiC_f/SiC composites in fusion energy applications, a method of joining components that satisfies the requirements of radiation resistance, mechanical integrity, desirable thermal properties, safety

during operation and maintenance or accident, and acceptable waste management characteristics is required. Joints made from SiC satisfy the above criteria, but practical and reliable methods of their production must be developed. The use of pre-ceramic polymers for joining offers a number of attractive features, such as easy application and low processing temperatures (<1200 °C for obtaining a dense ceramic layer) that inhibit fiber damage during joining, but several issues remain to be addressed.

The primary requirements for inorganic polymer, pre-ceramic precursors to be suitable for joining in fusion energy applications is that they must have high ceramic yield, minimal evolution of volatile decomposition products, optimal rheological properties, and practical curing characteristics. Precursor compositions with minimal evolution of gaseous species and low shrinkage, that can be handled and processed in ambient conditions, are highly desirable. Conditions where high shrinkage rates and increases in viscosity occur at the same time must be avoided to prevent stresses occurring due to constraints. The role of surface roughness, particularly in woven ceramic matrix composites, and the contact area between the joint and substrate requires further investigation. Although intrinsic and extrinsic variables influence the value of strength reported for polymer derived joints, many studies indicate that the use of pre-ceramic polymers is an attractive method for obtaining silicon carbide-based joints for fusion energy applications.

Comparative mechanical property tests (4-point bend at 25 °C) of butt-joints of SiC made with the pre-ceramic polymer allylhydridopolysilane (aHPCS) filled with SiC powder, reaction formed joint produced by a process called ARCJoinT and a reaction bonded SiC joint prepared by Busek Co. of Natick, Massachusetts revealed a wide range of joint strengths ranging from 53 to 134 MPa [46]. Joints made with a HPCS had an average strength of 80 MPa while joints made with ARCJoinT process had an average strength of 134 MPa but this increased to 247 MPa when tested at 1100 °C in air. A fourth joining method using an in-situ displacement reaction to produce a joint of $Ti_xSi_yC_z + SiC$ resulted in a joint strength of 187 MPa.

Riccardi et al. [47] evaluated a eutectic alloy of Si–22%Ti to braze both monolithic and composite SiC materials. The braze filler material was produced from powders of the eutectic that melts at 1330 °C and the joints produced in a vacuum and inert gas environments. Shear tests were performed at room temperature using the ASTM D905-89 method and gave shear strengths of 50 MPa for the monolithic SiC and up to 60 MPa for the composite material. Tests at 600 °C produced the same strength with the composite material and fracture occurred in the matrix and not the braze filler metal in both the monolithic and composite material. For comparison, Lewinsohn et al. [46] obtained a shear strength of 32 MPa for the material joined with the ARCJoinT process. The tensile strength of this joint measured by four point bend was 78 MPa. It will be necessary to correlate the ASTM D905-89 and asymmetric four point bend shear strengths before a conclusion can be reached regarding the differences in these two shear strength results.

6.7. Thermal and mechanical transient behavior

Transient thermal conditions will occur in a fusion energy system from both the system duty cycle and plasma discharge processes. Shutdown of the system for either scheduled or unscheduled maintenance will result in a temperature decrease of the blanket that inevitably will cause some stress build-up in the material. The stress magnitude will be dependent on the cooling rate and thermal gradients. This type of cycle is usually referred to as thermal-fatigue, involves the entire blanket and is measured in the laboratory in simulated thermal cycling tests or low-cycle fatigue (mechanical) tests. Start-up will also induce stress of the opposite sign to that produced by shutdown and may relax the cool-down stresses. Plasma discharge will induce a rapid heating of a small volume of plasma-facing material. Transmission of the thermal energy through the blanket and therefore the temperature change and stress response will be very design and material dependent.

Cooling the surface of a material faster than the interior results in a surface tensile stress while heating the surface of a material faster than the interior results in a surface compressive stress. The heating or cooling rate and temperature change determine the magnitude of the stress. The maximum temperature can also affect the material microstructure and properties. The magnitude of the stress is determined by the heating rate through the resulting thermal gradient. For thermal shock conditions the thermal diffusivity may be sufficiently slow that a thermal gradient is not established in the short-term such that the surface stress is determined by the energy deposition and resulting surface temperature and not by a thermal gradient. Assuming that the residual stresses have relaxed to zero at the operating temperature, cooling during a shutdown will result in a surface tensile stress and a plasma discharge in a surface compressive stress. In composite materials, internal stresses are also determined by the differential thermal expansion between the fiber and matrix so that the analysis of thermal stress is more complex than for a monolithic material. It is conceivable that the internal stresses could reverse the thermal gradient stress.

Jones [48] recently reviewed the limited database on thermal shock behavior of SiC_f/SiC composites. This data suggests continuous fiber ceramic matrix composites such as SiC_f/SiC exhibit very good thermal shock

characteristics but most data was obtained for a decrease in temperature ($-\Delta T$) as a result of quenching from an elevated temperature. Thermal shock in a fusion energy system will result from plasma discharge and will result in an increase in temperature ($+\Delta T$). One study was reported for SiC_f/SiC composites given $+\Delta T$ with no loss in strength following 25 cycles at a heating rate of 1700 K/s. Monolithic SiC failed in 1.5 cycles at a heating rate of 1400 K/s. Thermal fatigue test results reported by Jones and Henager [49] also suggest that SiC_f/SiC composites will exhibit little or no degradation for 100's of cycles.

7. Summary

Silicon carbide composites are specified in the TAURO, ARIES-AT and DREAM fusion reactor designs. The TAURO and ARIES-AT designs utilize a Pb–17%Li coolant while the DREAM reactor utilizes He as the coolant. Many of the design requirements, such as material operating temperature, thermal conductivity and strength, are similar for these designs with of course the exception in chemical compatibility between Pb–Li and He and SiC. The performance of current SiC_f/SiC composites are close to many of these requirements but a few fall short at least a factor of two. There have been further advancements in understanding radiation damage in SiC at the fundamental level through MD simulations of displacement cascades demonstrating the production of point defect clusters with general characteristics similar to metals. There has been a significant advancement in the radiation stability of composites made with the advanced fibers of Nicalon Type S and the UBE Tyranno SA. No change in strength was observed up to 10 dpa at 800 °C while earlier composites showed strength losses at less than one dpa. There have been advances in the development of materials with improved thermal conductivity and modeling thermal conductivity, joining and models for life-prediction. High transmutation rates of C and Si to form H, He, Mg and Al continue to be a concern but high-quality data to assess these effects awaits the availability of a high-energy neutron source.

References

[1] A.R. Raffray et al., Fus. Eng. Des. 55 (2001) 55.
[2] G. Aiello, H. Golfier, J.F. Marie, Y. Poitevin, J.F. Salavy, Fus. Eng. Des., in press.
[3] F. Gao, E.M. Bylaska, W.J. Weber, L.R. Corrales, Nucl. Instrum. and Meth. Phys. Res. B 180 (2001) 286.
[4] F. Gao, E.J. Bylaska, W.J. Weber, L.R. Corrales, Phys. Rev. B 64 (2001) 245208.
[5] W. Jiang, W.J. Weber, Phys. Rev. B 64 (2001) 125206.
[6] F. Gao, D.J. Bacon, Philos. Mag. A 71 (1995) 43.
[7] F. Gao, W.J. Weber, Phys. Rev. B 63 (2000) 054101.
[8] F. Gao, W.J. Weber, J. Appl. Phys. 89 (2001) 4275.
[9] F. Gao, R. Devanathan, W.J. Weber, Fus. Tech. 39 (2001) 574.
[10] R. Devanathan, W.J. Weber, F. Gao, J. Appl. Phys. 90 (2001) 2303.
[11] D.J. Bacon, A.F. Calder, F. Gao, V.G. Kapinos, S.J. Wooding, Nucl. Instrum. and Meth. Phys. Res. B 102 (1995) 37.
[12] F. Gao, W.J. Weber, W. Jiang, Phys. Rev. B 63 (2001) 214106.
[13] F. Gao, W.J. Weber, R. Devanathan, Nucl. Instrum. Meth. Phys. Res. B 180 (2001) 176.
[14] W.J. Weber, W. Jiang, S. Thevuthasan, Nucl. Instrum. Meth. Phys. Res. B (2001) 26.
[15] W.J. Weber, Nucl. Instrum. and Meth. Phys. Res. B 166–167 (2000) 98.
[16] F. Gao, W.J. Weber, Microstructural processes in irradiated materials, in: G.E. Lucas, S. Snead, M.A. Kirk, R.G. Elliman (Eds.), Materials Research Society Symposium Proceedings, vol. 650, Warrendale, PA, 2001, p. R3.201-6.
[17] F. Gao, W.J. Weber, J. Mater. Res. 17 (2002) 259.
[18] F. Gao, W.J. Weber, R. Devanathan, Nucl. Instrum. and Meth. Phys. Res. B 191 (2002) 487.
[19] W.J. Weber, L.M. Wang, Nucl. Instrum. and Meth. Phys. Res. B 106 (1995) 298.
[20] L.L. Snead, J. Nucl. Mater. 283–287 (2000) 551.
[21] T. Hinoki, PRICM4, 2001, to be presented.
[22] R.H. Jones, G.E. Youngblood, C.H. Henager Jr, M.L. Hamilton, H.L. Heinisch, C.A. Lewinsohn, Progress in the Development of SiC/SiC Composites for Fusion Energy Applications, in proceedings of the 1st IEA International Workshop on SiC/SiC Ceramic Composites for Fusion Structural Applications, Ispra, Italy, 19–28 October 1996, p. 1.
[23] L.L. Snead, J. Nucl. Mater., in press.
[24] T. Nozawa, Proceedings of the 10th International Conference on Fusion Reactor Materials, Baden–Baden, Germany, J. Nucl. Mater., in press.
[25] R.J. Price et al., J. Nucl. Mater. 108–109 (1982) 732.
[26] R.J. Price et al., J. Nucl. Mater. 33 (1969) 17.
[27] L.L. Snead, Proceedings of the 10 International Conference on Fusion Reactor Materials, Baden–Baden, Germany, J. Nucl. Mater., in press.
[28] D.A.G. Bruggemann, M. Annal. Physik. 24 (1935) 636.
[29] S. Nomura, T.W. Chou, J. Comp. Mater. 14 (1980) 120.
[30] J.J. Brennan, L.D. Bentsen, D.P.H. Hasselman, J. Mater. Sci. 17 (1982) 2337.
[31] H. Tawil, L.D. Bentsen, S. Baskaran, D.P.H. Hasselman, J. Mater. Sci. 20 (1985) 3201.
[32] D.P.H. Hasselman, L.F. Johnson, R. Syed, M.P. Taylor, K. Chyung, J. Mater. Sci. 22 (1987) 701.
[33] D.P.H. Hasselman, A. Venkateswaran, M. Yu, H. Tawil, J. Mater. Sci. Lett. 10 (1991) 1037.
[34] H. Bhatt, K.Y. Donaldson, D.P.H. Hasselman, J. Am. Ceram. Soc. 75 (1992) 334.
[35] D.P.H. Hasselman, L.F. Johnson, J. Comp. Mater. 21 (1987) 508.
[36] R.H. Jones, Environmental Effects On SiC/SiC Composites For Fusion Structural Applications, Fusion Reactor

Materials Semi-Annual Progress Report for period ending March 31, 1991, DOE/ER-0313/10, p. 215.
[37] T. Sample, P. Fenici, H. Kolbe, L. Orecchia, J. Nucl. Mater 212–215 (1994) 1529.
[38] R.H. Jones, C.H. Henager Jr, C.F. Windisch Jr, Mater. Sci. Eng. A 198 (1995) 103.
[39] R.H. Jones, C.H. Henager Jr, C.A. Lewinsohn, C.F. Windisch Jr, J. Am. Ceram. Soc. 83 (2000) 1999.
[40] P. Fenici, H.W. Scholz, J. Nucl. Mater. 212–215 (1994) 60.
[41] H. Kleykamp, Ber. Bunsenges. Phy. Chem. 102 (1998) 1231.
[42] T. Terai, T. Yoneoka, S. Tanak, Compatibility test of SiC with liquid metal breeders, International Town Meeting on SiC/SiC Design and Material Issues for Fusion Systems, Oak Ridge National Laboratory, 18–19 January 2000.
[43] S.J. Zinkle, N.M. Ghoniem, Fus. Eng. Des. 51&52 (2000) 55.
[44] C.H. Henager Jr, C.A. Lewinsohn, R.H. Jones, Acta Mater. 49 (2001) 3727.
[45] C.H. Henager Jr, R.G. Hoagland, Acta Mater. 49 (2002) 3739.
[46] C.A. Lewinsohn, R.H. Jones, M. Singh, T. Nozawa, M. Kotani, Y. Katoh, A. Kohyama, Proceedings of the 10th International Conference on Fusion Reactor Materials, Baden–Baden, Germany, J. Nucl. Mater., in press.
[47] B. Riccardi, C.A. Nannetti, T. Petrisor, M. Sacchetti, Proceedings of the 10th International Conference on Fusion Reactor Materials, Baden–Baden, Germany, J. Nucl. Mater., in press.
[48] R.H. Jones, Response of SiC/SiC to Transient Thermal Conditions: A Review, in: Fusion Materials Semiannual Progress Report for period ending June 30, 2001, DOE/ER-0313/30, p. 45.
[49] R.H. Jones, C.H. Henager Jr, J. Nucl. Mater. 219 (1995) 55.